

Emergence of Spin Ice freezing in $\text{Dy}_2\text{Ti}_{1.8}\text{Mn}_{0.2}\text{O}_7$

Rajnikant Upadhyay,¹ Manjari Shukla,¹ Rachana Sain,¹ Martin Tolkiehn,² and Chandan Upadhyay¹

¹*School of Materials Science and Technology, Indian Institute of Technology (Banaras Hindu University), Varanasi 221005, India*

²*Deutsches Elektronen-Synchrotron (DESY), Notkestraße 85, 22607, Hamburg, Germany*

We herein present the spin freezing dynamics of stuffed polycrystalline compound $\text{Dy}_2\text{Ti}_{1.8}\text{Mn}_{0.2}\text{O}_7$. In $\text{Dy}_2\text{Ti}_2\text{O}_7$, spin freezes with ice like spin relaxations at a temperature around 3 K (T_i) along with another spin freezing at a temperature around 0.7 K ($T < T_i$). These relaxations can be observed prominently with an application of varying DC magnetic field bias and applied AC-field. We show here that with fractional inclusion of Mn at Ti site in $\text{Dy}_2\text{Ti}_2\text{O}_7$, there is a significant shift in these temperatures. In $\text{Dy}_2\text{Ti}_{1.8}\text{Mn}_{0.2}\text{O}_7$ the T_i shifts to a higher temperature around 5 K and freezing belonging to $T < T_i$ shifts to 2.5 K without any application of external DC Bias and/or AC-field. The inclusion of Mn at Ti site also enhances the ferromagnetic interaction for $\text{Dy}_2\text{Ti}_{1.8}\text{Mn}_{0.2}\text{O}_7$ as compared to $\text{Dy}_2\text{Ti}_2\text{O}_7$. Arrhenius fit of freezing temperature with frequency for $\text{Dy}_2\text{Ti}_{1.8}\text{Mn}_{0.2}\text{O}_7$ shows that these spin relaxations at T_i and $T < T_i$ are thermally induced. Low-temperature structural change in lattice parameters and crystal field phonon coupling has been studied using synchrotron x-ray diffraction. Debye-Gruineisen analysis of temperature-dependent lattice volume shows the emergence of crystal field phonon coupling at a much higher temperature (70 K) in $\text{Dy}_2\text{Ti}_{1.8}\text{Mn}_{0.2}\text{O}_7$ in contrast to 40 K in $\text{Dy}_2\text{Ti}_2\text{O}_7$. These findings make $\text{Dy}_2\text{Ti}_{1.8}\text{Mn}_{0.2}\text{O}_7$ a suitable system to explore the application of spin ice phenomenon at a workable temperature.

I. INTRODUCTION

Geometric frustration in a magnetic system occurs when the spatial arrangement of the magnetic moments (“spins”) combined with the magnetic interactions prevents the formation of a “simple” ordered ground state. Rare earth pyrochlores $\text{A}_2\text{B}_2\text{O}_7$, where A is a trivalent ion and B is tetravalent ion, belongs to class of frustrated materials in which geometry of the magnetic sublattice leads to frustration [1]. It displays a wide variety of unconventional and exciting magnetic ground states from spin liquid to spin glass through spin ice behaviour [2–4]. For the spin ice compounds the near neighbour interactions between the Ising spins are dipolar ferromagnetic (FM) and weaker antiferromagnetic (AFM) exchange. Overall, this configuration results in effective frustrated ferromagnetic interaction in order to minimize the dipolar and ferromagnetic exchange interaction to attain the ground state, spins on each tetrahedron adopt the two-in-two-out configuration, which is analogous to the two-short-two-long proton bond configuration in water ice [5]. These interaction results in six-fold degenerate ground state, which gives residual measurable zero-point entropy $S_0 = R/2\ln(3/2)$, where R is the molar gas constant [6]. A brief history of spin ice has been summarised by Bramwell and Harris [7]

Spin ice materials $\text{Dy}_2\text{Ti}_2\text{O}_7$, $\text{Ho}_2\text{Ti}_2\text{O}_7$, $\text{Dy}_2\text{Sn}_2\text{O}_7$ and $\text{Ho}_2\text{Sn}_2\text{O}_7$, in which lattice geometry leads to frustration due to competing ferromagnetic and dipolar interactions, have shown a rich physics originating from its inherent geometric frustration and resultant highly degenerate ground state [6, 8, 9]. The structure is represented by the space group $\text{Fd}\bar{3}\text{m}$ featuring two sublattices that interpenetrate each other and consist of networks of corner-sharing tetrahedra. The magnetic rare-earth ion resides on the lattice of corner-sharing tetrahedra, where spin are constrained by crystal field to point

either directly toward or directly away from the centre of the tetrahedra. Specifically, for the pyrochlores with Dy and Ho at the A site, the rare-earth ion is subject to a strong crystal-electric-field splitting of the ground state and the first excited state of the single ion by an energy of the order of 200 K [10, 11]. In $\text{Dy}_2\text{Ti}_2\text{O}_7$, three relaxation phenomena have been observed, associated with single-spin relaxation at higher temperatures and spin with ice like correlations at lowest temperatures, but with quantum spin relaxation observed at intermediate temperatures. [12–15].

To examine the development of the magnetic ground state of stuffed spin ice. In the present study, we have used dc and ac magnetic susceptibility to investigate the nature of magnetic interaction and spin relaxation in thermal and quantum spin relaxation regimes by inclusion of small fraction of Mn at the Ti site, in the spin ice compound $\text{Dy}_2\text{Ti}_2\text{O}_7$ within the domain of phase space. It has been shown that spin ice freezing temperature shifts to higher temperature with the inclusion of Mn. This suggests that a relatively low level of inclusion of Mn at Ti site changing the number and type of relaxation processes available to the spin and freezing temperature in such system, making it interesting to study how low-temperature magnetic interaction evolves with Mn substitution at Ti site in $\text{Dy}_2\text{Ti}_2\text{O}_7$.

II. EXPERIMENTAL

Polycrystalline $\text{Dy}_2\text{Ti}_2\text{O}_7$ and $\text{Dy}_2\text{Ti}_{1.8}\text{Mn}_{0.2}\text{O}_7$ samples were prepared using the standard solid-state thermochemical reaction method [16]. The starting materials for synthesis was Dy_2O_3 , TiO_2 and MnO_2 sample was heated in ambient conditions at 1400 °C with multiple heating and grinding until the reaction was complete. High-resolution X-ray diffraction demonstrated the samples to be in single-phase pyrochlore. We measured dc susceptibility, as well as the real and imaginary part of

ac susceptibility, $\chi'(T)$ and $\chi''(T)$ applying excitation field $H_{ac} = 2.5$ Oe at different dc bias field using Quantum design MPMS superconducting quantum interference device magnetometer. Synchrotron x-ray diffraction (SXRD) has been carried out to investigate the structural changes at low temperatures using P24 beamline at Petra III at DESY, Hamburg, Germany. The diffraction pattern was obtained using a 25 KeV x-ray radiation source in the temperature range of (15-140) K with a Q value ranging from 0.2 to 7.5. Rietveld refinement for the obtained SXRD was performed using FULLPROF SUIT [17].

III. RESULTS AND DISCUSSION

The static magnetization was measured using zero field cooling and field cooling protocol in the temperature range from 2 K to 200 K at a rate of 2 K. FIG.1(a)

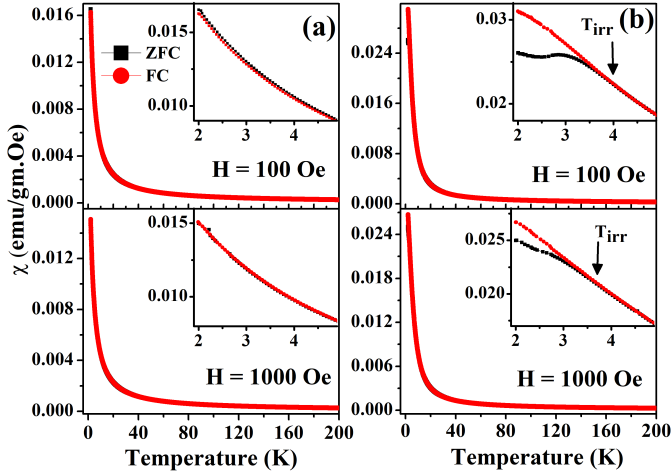


FIG. 1. Temperature dependence of magnetization measured in ZFC and FC protocol for (a) $Dy_2Ti_2O_7$ and (b) $Dy_2Ti_{1.8}Mn_{0.2}O_7$ at an applied field of 100 Oe and 1000 Oe.

shows zero field cooled (ZFC) and field Cooled (FC) magnetization data for $Dy_2Ti_2O_7$. There is no difference in ZFC and FC curve in the measured temperature range, suggesting no magnetic ordering or absence of spin-glass like transition down up to 2 K as reported earlier [18]. However, the dc magnetic susceptibility shows clear bifurcation in ZFC and FC for $Dy_2Ti_{1.8}Mn_{0.2}O_7$ at a lower temperature around 3.8 K (FIG.1(b)). The irreversibility in ZFC and FC signifies enhanced ferromagnetism which is expected because of increasing disorder [19]. We have also seen the effects of applied magnetic field on freezing temperature i.e bifurcation point. FIG.2 shows that bifurcation temperature (T_{irr}) decreases with an increase in the magnetic field from 50 Oe to 1500 Oe; as expected for materials lacking long-range magnetic ordering [19]. This behaviour is similar to typical spin-glass system i.e. monotonic decrease of ZFC curve below T_{irr} and also with the increase in the applied field, the percentage difference between two ZFC and FC data set decreases. With further increase in the field above 1500 Oe no difference in ZFC and FC curve is observed [13].

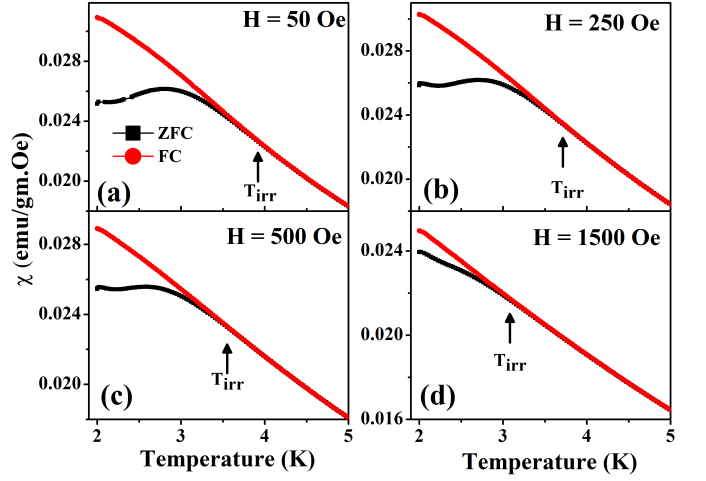


FIG. 2. Temperature dependence of magnetization measured in ZFC and FC protocol for $Dy_2Ti_{1.8}Mn_{0.2}O_7$ at applied field of (a) 50 Oe (b) 250 Oe (c) 500 Oe (d) 1500 Oe.

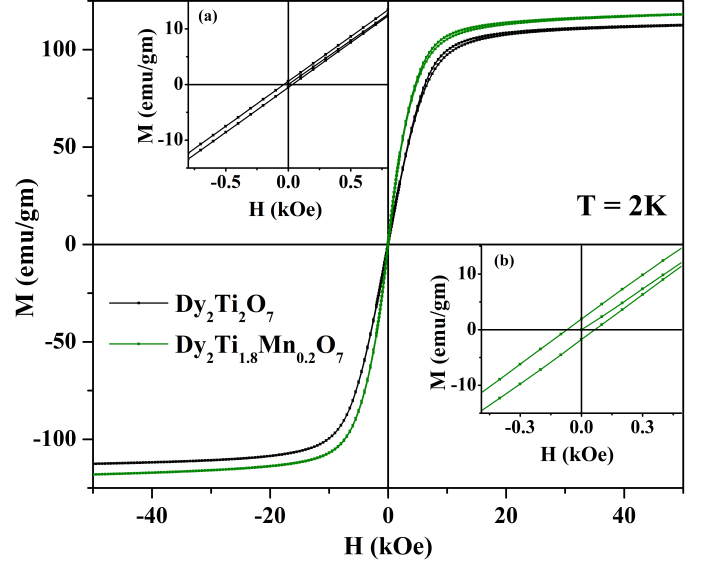


FIG. 3. Magnetization as a function of Field (MH) curve for $Dy_2Ti_2O_7$ and $Dy_2Ti_{1.8}Mn_{0.2}O_7$ at 2K for H (magnetic field) ranging from -50 to 50 kOe.

FIG.3 show the field dependence of magnetization (M - H) curve measured at 2K; the field was swept upto 5 kOe, down to -5 kOe, and back upto 5 kOe to complete the hysteresis loop. M_{max} value calculated from the M - H plot is $42.72 \mu_B$ /unit cell in the case of $Dy_2Ti_2O_7$, which is consistent with previously reported value. The M_{max} value increases to $44.776 \mu_B$ /unit cell for $Dy_2Ti_{1.8}Mn_{0.2}O_7$ [20, 21]. The obtained value is half of the actual magnetic moment of due to the angular averaging in case of the powdered sample. The saturation value of magnetization shows a slight increase in M_{max} value for $Dy_2Ti_{1.8}Mn_{0.2}O_7$, indicating that inclusion does not measurably alter the system's anisotropy [15]. The magnetization increases upto 20 kOe and then

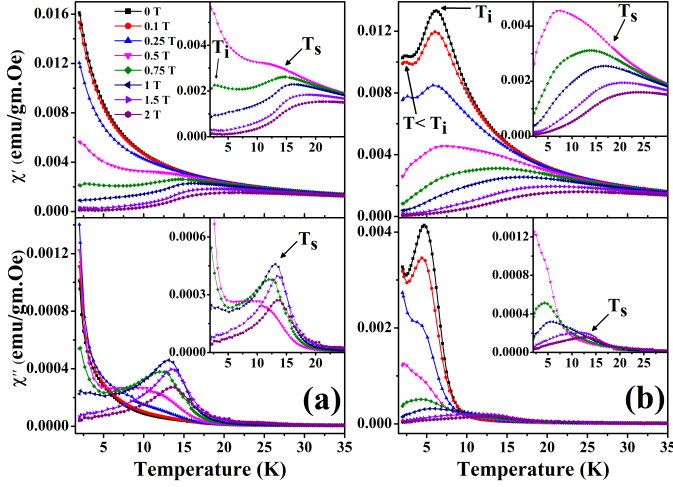


FIG. 4. The real (upper panel) and imaginary part (lower panel) of ac susceptibility at several applied dc magnetic fields and at frequency of 300 Hz for (a) $\text{Dy}_2\text{Ti}_2\text{O}_7$ (b) $\text{Dy}_2\text{Ti}_{1.8}\text{Mn}_{0.2}\text{O}_7$.

remains saturated upto an applied field of 50 kOe.

The evidence of bifurcation in the MT plot for $\text{Dy}_2\text{Ti}_{1.8}\text{Mn}_{0.2}\text{O}_7$ at measured temperature made us probe into the system's spin dynamics. Since there is a bifurcation in the dc susceptibility plot, we expect freezing above this temperature in ac susceptibility data. FIG.4 shows real and imaginary part of field-dependence ac susceptibility measurement at a frequency of 300 Hz and DC bias magnetic field ranging from 0-2 T. The real part of ac susceptibility is virtually identical to dc susceptibility in case of $\text{Dy}_2\text{Ti}_2\text{O}_7$, in the absence of an applied dc field, FIG.4(a). With increasing the field after 0.25 T we see the emergence of two relaxations, one corresponding to single ion freezing temperature (T_s) at around 15 K [15] and a spin ice state that emerges around 3 K (T_i) [22] appears in real part of ac susceptibility $\chi'(T)$, we also observe peak in $\chi''(T)$ corresponding to maximum in $\chi'(T)$ as expected from Kramer-Kronig relation [13, 23]. The freezing at higher temperature become more pronounced with increase in the field which is the characteristics for spin ice, whereas for spin glasses and superparamagnets magnetic field suppresses the freezing temperature [24, 25]. The single-ion freezing (T_s) shifts towards higher temperature with increase in magnetic field. Such behavior has been observed by Shi et al. in ac susceptibility measurements performed on single crystal of $\text{Dy}_2\text{Ti}_2\text{O}_7$ [26]. Whereas in case of $\text{Dy}_2\text{Ti}_{1.8}\text{Mn}_{0.2}\text{O}_7$, FIG.4(b), there appears two relaxation at a lower temperature near spin ice state even in the absence of dc field first one around 4 K (T_i) and another one below T_i at around 2.5 K ($T < T_i$). The one which is around 2.5 K ($T < T_i$) can be correlated to the low temperature freezing which comes at around 0.7 K in $\text{Dy}_2\text{Ti}_2\text{O}_7$ which is studied in detail by Snyder et al. [13]. It Suggests that the inclusion of Mn shifts the spin ice freezing state to higher temperature. Further with increase in the field the single ion freezing (T_s) appears and the one at lowest temper-

ature ($T < T_i$) disappears. Real part of ac susceptibility $\chi'(T)$ shows suppression in higher temperature freezing (T_s) in case of $\text{Dy}_2\text{Ti}_{1.8}\text{Mn}_{0.2}\text{O}_7$ when we increase the field above 0.5 T. To analyze the role of Mn, ac susceptibility for both the compound are plotted in single figure at various applied field, FIG.5. FIG.5(a) shows spin ice freezing in $\text{Dy}_2\text{Ti}_{1.8}\text{Mn}_{0.2}\text{O}_7$ at zero dc bias which is not observed in $\text{Dy}_2\text{Ti}_2\text{O}_7$. As shown in FIG.5(b) T_s is suppressed at an applied dc field of 0.5 T. As we increase the applied field to 0.75 T the freezing at lower temperature T_i merges with T_s and gives a single hump like feature FIG.5(c). Further with increase of field to 2 T both $\text{Dy}_2\text{Ti}_2\text{O}_7$ and $\text{Dy}_2\text{Ti}_{1.8}\text{Mn}_{0.2}\text{O}_7$ shows similar behaviour FIG.5(f). This shows that substitution of Mn alters the spin dynamics of the system at lower temperature regime i.e near spin ice state and higher temperature regime, near single ion freezing temperature in different way.

To examine the nature of freezing phenomena, ac susceptibility data is collected in the vicinity of low temperature at varying frequencies ranging from 50 Hz to 700 Hz at various applied dc fields. FIG.6 shows the temperature dependent susceptibility as a function of frequency for both the compounds in absence of applied dc field. The real part of ac susceptibility measurement $\chi'(T)$ shows canonical paramagnetic type behaviour for $\text{Dy}_2\text{Ti}_2\text{O}_7$ for all applied frequencies ($f = 50, 100, 200, 300, 500, 700$ Hz) corresponding to which there is sharp

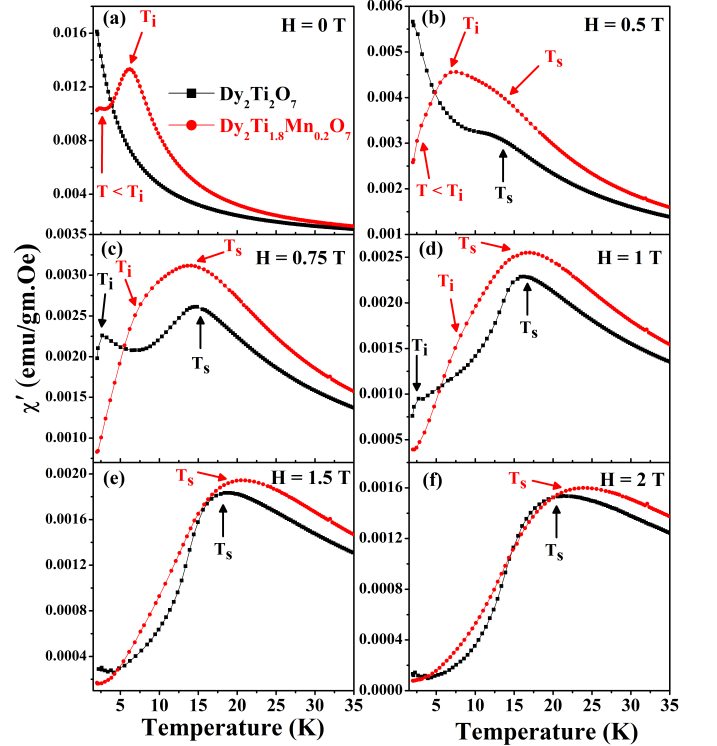
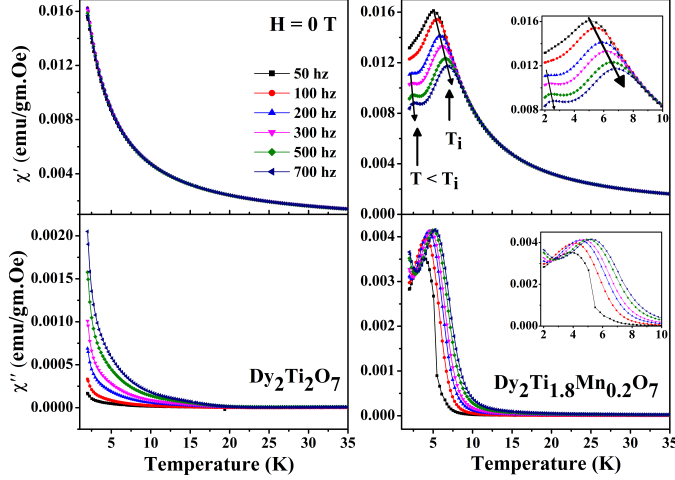
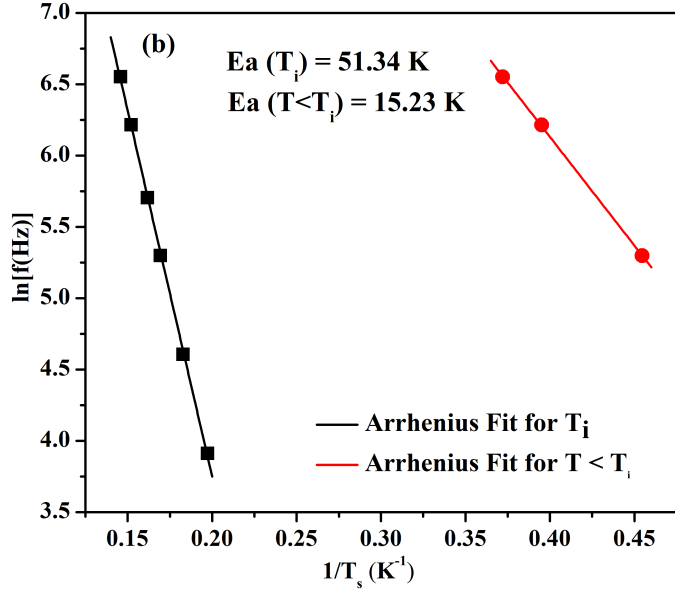


FIG. 5. Temperature dependence of the real part of ac susceptibility measured at the 300 Hz frequency for $\text{Dy}_2\text{Ti}_2\text{O}_7$ and $\text{Dy}_2\text{Ti}_{1.8}\text{Mn}_{0.2}\text{O}_7$ at different DC bias fields (a) 0 T (b) 0.5 T (c) 0.75 T (d) 1 T (e) 1.5 T (f) 2 T

TABLE I. The parameters $V(T = 0)$, θ_D and $9\gamma Nk_B/B$ for $\text{Dy}_2\text{Ti}_2\text{O}_7$ and $\text{Dy}_2\text{Ti}_{1.8}\text{Mn}_{0.2}\text{O}_7$ obtained by fitting Debye Function.

Compound	$V(T = 0\text{K}) (\text{\AA}^3)$	Debye temperature, $\theta_D(\text{K})$	$9\gamma Nk_B/B (\text{\AA}^3 / \text{K})$
$\text{Dy}_2\text{Ti}_2\text{O}_7$	1034.7	214.1	0.065
$\text{Dy}_2\text{Ti}_{1.8}\text{Mn}_{0.2}\text{O}_7$	1032.3	290.6	0.066

FIG. 6. Frequency dependence for $\text{Dy}_2\text{Ti}_2\text{O}_7$ and $\text{Dy}_2\text{Ti}_{1.8}\text{Mn}_{0.2}\text{O}_7$ at an applied field of 0 TFIG. 7. Arrhenius law fit of freezing temperatures (T_i and $T < T_i$) dependence on frequency for $\text{Dy}_2\text{Ti}_{1.8}\text{Mn}_{0.2}\text{O}_7$

increase in the imaginary part $\chi''(T)$ in the lower panel as well. Whereas for $\text{Dy}_2\text{Ti}_{1.8}\text{Mn}_{0.2}\text{O}_7$, we see that both lower temperature spin ice freezing which is around 4 K (T_i) and 2.5 K ($T < T_i$) shows strong frequency dependence. To investigate the nature of T_i and ($T < T_i$) as well as the spin dynamics in $\text{Dy}_2\text{Ti}_{1.8}\text{Mn}_{0.2}\text{O}_7$, we examine the frequency dependence of T_i and ($T < T_i$) by

fitting the data to an Arrhenius law given below

$$f = f_0 e^{\frac{E_A}{K_B T}} \quad (1)$$

Where E_A is the activation energy for spin fluctuations, K_B is Boltzmann constant and f_0 is a measure of the microscopic limiting frequency in the system [15]. FIG.7 shows the Arrhenius fit, the activation energy comes out to be 51.34 K for spin relaxation at T_i and 15.23 K for the spin relaxation at $T < T_i$ in case of $\text{Dy}_2\text{Ti}_{1.8}\text{Mn}_{0.2}\text{O}_7$, it seems that activation energy has been increased for spin relaxation at T_i which is expected as lattice constant has decreased [15]. The Arrhenius law behaviour indicates that spin relaxation are thermally driven [14]. The values of the freezing temperature are obtained from the minimum in the slope of $\chi'(T)$ with Mn substitution T_i and ($T < T_i$) shifts towards the higher temperature side with increase in frequency this peak shift towards higher temperature.

SXRD was performed from 140 K to 15 K at an interval of 10 K, to establish the Crystal field phonon coupling. FIG.8 shows the some selected low-temperature SXRD pattern for $T = 140$ K, 60 K, 30 K, 15 K and its rietveld refinement. Temperature-dependent variation of lattice volume has been plotted. Debye Gruineisen equation has been fitted to extract the crystal field-induced change in the lattice volume. The equation is as follows:

$$V \cong V(T = 0) + \int_0^T \frac{\gamma C_v}{B} dT$$

$$V \cong V(T = 0) + \frac{9\gamma Nk_B}{B} T \left(\frac{T}{\theta_D} \right)^3 \int_0^{\frac{\theta_D}{T}} \frac{e^x}{e^x - 1} dx \quad (2)$$

$V(T=0)$, θ_D and $9\gamma Nk_B/B$ are fitting parameters; $V(T = 0)$ represents the lattice volume at 0 K, θ_D is the Debye temperature, γ is Grüneisen parameter and B is the bulk modulus [27, 28]. Debye model accounts for contribution to thermal expansion due to anharmonic parts of lattice vibration. As shown in FIG.9(a) lattice volume decreases linearly till 40 K, below which it shows apparent deviation from Debye Gruineisen fit, showing the dominance of crystal field at low temperature in case of $\text{Dy}_2\text{Ti}_2\text{O}_7$, but for $\text{Dy}_2\text{Ti}_{1.8}\text{Mn}_{0.2}\text{O}_7$ (FIG.9(b)), lattice volume decreases as per Debye equation till 70 K then it deviates and becomes somewhat constant then again it drops below 40 K this suggests that with Mn substitution crystal field prominence starts at higher temperature (70 K). The obtained value of $V(T = 0)$, θ_D and $9\gamma Nk_B/B$, fitting parameters are depicted in the Table 1.

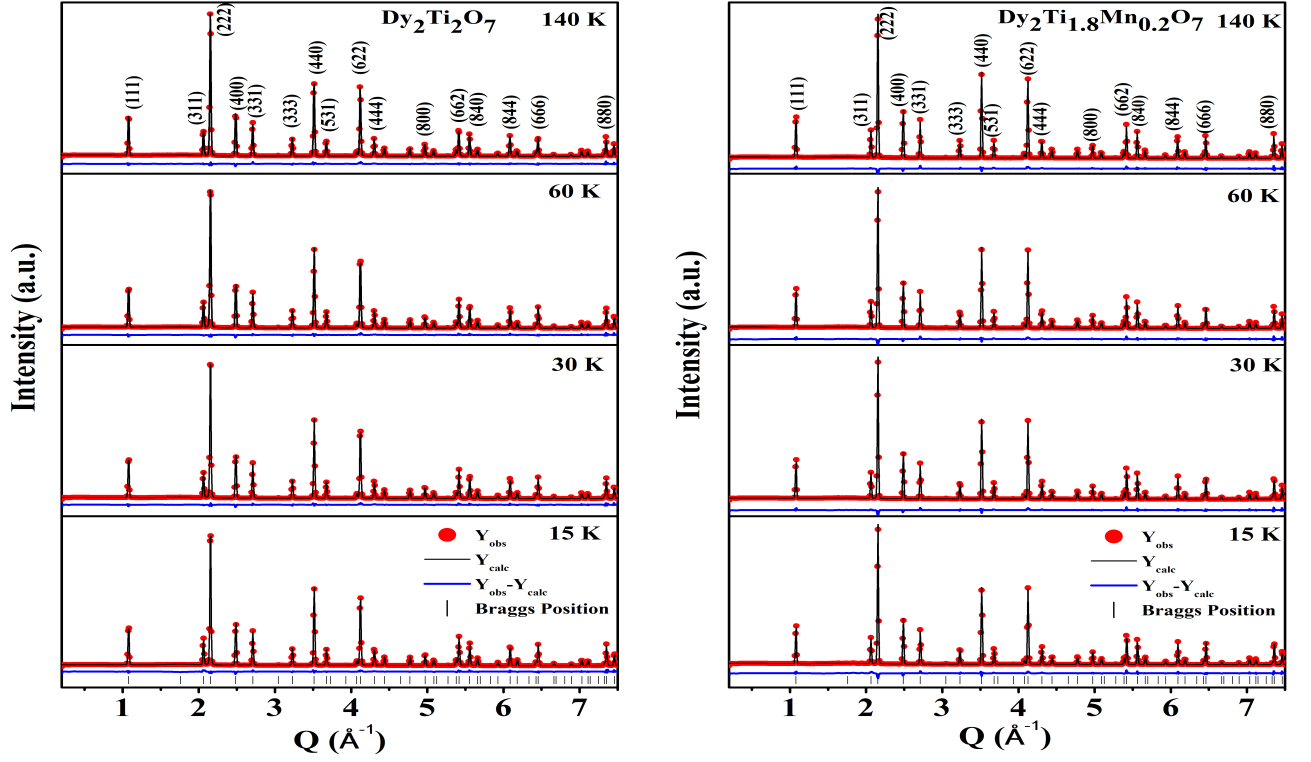


FIG. 8. Rietveld refinement of low temperature synchrotron x-ray diffraction pattern of $\text{Dy}_2\text{Ti}_2\text{O}_7$ and $\text{Dy}_2\text{Ti}_{1.8}\text{Mn}_{0.2}\text{O}_7$ at $T = 140$ K, $T = 60$ K, $T = 30$ K and $T = 15$ K.

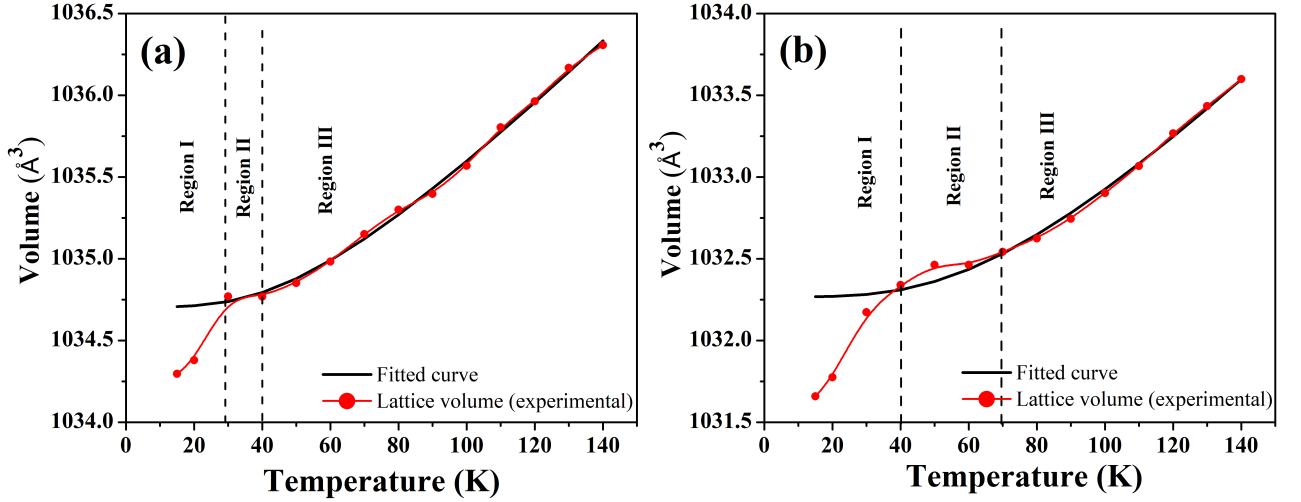


FIG. 9. Temperature variations of unit cell parameters solid line (black) represent the fitted curve contribution of phonons by Debye Gruineisen, and solid circle (red) represents experimental lattice volume (a) $\text{Dy}_2\text{Ti}_2\text{O}_7$ and (b) $\text{Dy}_2\text{Ti}_{1.8}\text{Mn}_{0.2}\text{O}_7$.

It shows the enhancement in Debye temperature with Mn inclusion at Ti site to $\theta_D = 290.6$ for $\text{Dy}_2\text{Ti}_{1.8}\text{Mn}_{0.2}\text{O}_7$ in comparison to $\theta_D = 214.1$ for $\text{Dy}_2\text{Ti}_2\text{O}_7$. Such an enhancement shows the increase in the crystal field energy dominance to set in at higher temperature in case of $\text{Dy}_2\text{Ti}_{1.8}\text{Mn}_{0.2}\text{O}_7$ at 70 K.

IV. CONCLUSIONS

We have studied low temperature magnetic ordering and spin dynamics for the polycrystalline com-

pound $\text{Dy}_2\text{Ti}_{1.8}\text{Mn}_{0.2}\text{O}_7$. With small Mn inclusion at Ti site in $\text{Dy}_2\text{Ti}_2\text{O}_7$, We observe an emergence of a low-temperature spin ice freezing relaxation around 5 K (T_i) along with the second spin relaxation feature around 2.5 K ($T < T_i$) even in absence of any dc magnetic field which was not observed in case of $\text{Dy}_2\text{Ti}_2\text{O}_7$. Both the spin relaxations at T_i and $T < T_i$ shows strong frequency dependence and Arrhenius fit shows that these spin relaxation are thermally driven. Mn is altering the spin dynamics

of $\text{Dy}_2\text{Ti}_2\text{O}_7$ at low temperature regime. The low temperature Synchrotron x-ray diffraction study confirms absence of structural phase transition in this system. Debye parameters calculated by fitting Temperature-dependent variation of lattice volume using Debye Gruineisen equation. It shows that crystal field energy dominance set in at higher temperatures in case of $\text{Dy}_2\text{Ti}_{1.8}\text{Mn}_{0.2}\text{O}_7$ in comparison to $\text{Dy}_2\text{Ti}_2\text{O}_7$. Such a small perturbation in the composition makes this system suitable for applications, where spin ice like freezing needed to be explored

at a workable temperatures.

V. ACKNOWLEDGEMENTS

We acknowledge CIFIC, IIT (BHU) for magnetic measurements. The Synchrotron XRD was carried out at PETRA III of DESY, a member of the Helmholtz Association (HGF). Financial support by the Department of Science and Technology (Government of India) provided within the framework of the India@DESY collaboration is gratefully acknowledged.

-
- [1] M. Subramanian and A. Sleight, Rare earth pyrochlores, Handbook on the physics and chemistry of rare earths **16**, 225 (1993).
 - [2] J. S. Gardner, M. J. Gingras, and J. E. Greedan, Magnetic pyrochlore oxides, Rev. Mod. Phys. **82**, 53 (2010).
 - [3] J. E. Greedan, Frustrated rare earth magnetism: Spin glasses, spin liquids and spin ices in pyrochlore oxides, J. Alloys Compd. **408**, 444 (2006).
 - [4] L. Balents, Spin liquids in frustrated magnets, Nature **464**, 199 (2010).
 - [5] M. J. Harris, S. Bramwell, D. McMorrow, T. Zeiske, and K. Godfrey, Geometrical frustration in the ferromagnetic pyrochlore $\text{Ho}_2\text{Ti}_2\text{O}_7$, Phys. Rev. Lett. **79**, 2554 (1997).
 - [6] S. T. Bramwell and M. J. Gingras, Spin ice state in frustrated magnetic pyrochlore materials, Science **294**, 1495 (2001).
 - [7] S. T. Bramwell and M. J. Harris, The history of spin ice, J. Phys. Condens. Matter **32**, 374010 (2020).
 - [8] A. P. Ramirez, A. Hayashi, R. J. Cava, R. Siddharthan, and B. Shastri, Zero-point entropy in ‘spin ice’, Nature **399**, 333 (1999).
 - [9] R. Siddharthan, B. Shastri, A. Ramirez, A. Hayashi, R. Cava, and S. Rosenkranz, Ising pyrochlore magnets: Low-temperature properties, “ice rules,” and beyond, Phys. Rev. Lett. **83**, 1854 (1999).
 - [10] K. Matsuhira, Y. Hinatsu, and T. Sakakibara, Novel dynamical magnetic properties in the spin ice compound $\text{Dy}_2\text{Ti}_2\text{O}_7$, J. Phys. Condens. Matter **13**, L737 (2001).
 - [11] S. Rosenkranz, A. Ramirez, A. Hayashi, R. Cava, R. Siddharthan, and B. Shastri, Crystal-field interaction in the pyrochlore magnet $\text{Ho}_2\text{Ti}_2\text{O}_7$, J. Appl. Phys. **87**, 5914 (2000).
 - [12] J. Snyder, J. Slusky, R. Cava, and P. Schiffer, How ‘spin ice’ freezes, Nature **413**, 48 (2001).
 - [13] J. Snyder, B. Ueland, J. Slusky, H. Karunadasa, R. Cava, and P. Schiffer, Low-temperature spin freezing in the $\text{Dy}_2\text{Ti}_2\text{O}_7$ spin ice, Phys. Rev. B. **69**, 064414 (2004).
 - [14] J. Snyder, B. Ueland, J. Slusky, H. Karunadasa, R. J. Cava, A. Mizel, and P. Schiffer, Quantum-classical reentrant relaxation crossover in $\text{Dy}_2\text{Ti}_2\text{O}_7$ spin ice, Phys. Rev. Lett. **91**, 107201 (2003).
 - [15] J. Snyder, B. Ueland, A. Mizel, J. Slusky, H. Karunadasa, R. Cava, and P. Schiffer, Quantum and thermal spin relaxation in the diluted spin ice $\text{Dy}_{2-x}\text{M}_x\text{Ti}_2\text{O}_7$ ($m = \text{Lu, Y}$), Phys. Rev. B. **70**, 184431 (2004).
 - [16] M. Shukla, R. Upadhyay, M. Tolkehn, and C. Upadhyay, Robust spin-ice freezing in magnetically frustrated $\text{Ho}_2\text{Ge}_x\text{Ti}_{2-x}\text{O}_7$ pyrochlore, J. Phys. Condens. Matter **32**, 465804 (2020).
 - [17] J. Rodriguez-Carvajal, An introduction to the program fullprof, Laboratoire Leon Brillouin (CEA-CNRS) (2001).
 - [18] H. Liu, Y. Zou, L. Zhang, L. Ling, H. Yu, L. He, C. Zhang, and Y. Zhang, Magnetic order and dynamical properties of the spin-frustrated magnet $\text{Dy}_{2-x}\text{Yb}_x\text{Ti}_2\text{O}_7$, J. Magn. Magn. Mater. **349**, 173 (2014).
 - [19] H. Liu, Y. Zou, L. Ling, L. Zhang, C. Zhang, and Y. Zhang, Enhanced ferromagnetism and emergence of spin-glass-like transition in pyrochlore compound $\text{Dy}_2\text{Ti}_{2-x}\text{V}_x\text{O}_7$, J. Magn. Magn. Mater. **388**, 135 (2015).
 - [20] V. Anand, D. Tennant, and B. Lake, Investigations of the effect of nonmagnetic Ca substitution for magnetic Dy on spin-freezing in $\text{Dy}_2\text{Ti}_2\text{O}_7$, J. Phys. Condens. Matter **27**, 436001 (2015).
 - [21] H. Fukazawa, R. Melko, R. Higashinaka, Y. Maeno, and M. Gingras, Magnetic anisotropy of the spin-ice compound $\text{Dy}_2\text{Ti}_2\text{O}_7$, Phys. Rev. B. **65**, 054410 (2002).
 - [22] X. Ke, R. Freitas, B. Ueland, G. Lau, M. Dahlberg, R. Cava, R. Moessner, and P. Schiffer, Nonmonotonic zero-point entropy in diluted spin ice, Phys. Rev. Lett. **99**, 137203 (2007).
 - [23] H. Xing, M. He, C. Feng, H. Guo, H. Zeng, and Z.-A. Xu, Emergent order in the spin-frustrated system $\text{Dy}_x\text{Tb}_{2-x}\text{Ti}_2\text{O}_7$ studied by ac susceptibility measurements, Phys. Rev. B. **81**, 134426 (2010).
 - [24] J. Gardner, B. Gaulin, S.-H. Lee, C. Broholm, N. Raju, and J. Greedan, Glassy statics and dynamics in the chemically ordered pyrochlore antiferromagnet $\text{Y}_2\text{Mo}_2\text{O}_7$, Phys. Rev. Lett. **83**, 211 (1999).
 - [25] J. A. Mydosh, *Spin glasses: an experimental introduction* (CRC Press, 1993).
 - [26] J. Shi, Z. Tang, B. Zhu, P. Huang, D. Yin, C. Li, Y. Wang, and H. Wen, Dynamical magnetic properties of the spin ice crystal $\text{Dy}_2\text{Ti}_2\text{O}_7$, J. Magn. Magn. Mater. **310**, 1322 (2007).
 - [27] E. Yakub, The modified debye-grüneisen model for highly compressed diamond, J. Low Temp. Phys. **187**, 20 (2017).
 - [28] T. Kiyama, K. Yoshimura, K. Kosuge, Y. Ikeda, and Y. Bando, Invar effect of SrRuO_3 : Itinerant electron magnetism of Ru 4d electrons, Phys. Rev. B. **54**, R756 (1996).